





Article

Origin and distribution of clay minerals in semi-arid Sahelian soils: case of Kori Ouallam watershed, south-western Niger

Salifou Noma Adamou¹ , Lahcen Daoudi², Amadou Abdourhamane Touré¹ and Nathalie Fagel³ 

¹Université Abdou Moumouni, Faculté des Sciences et Techniques, Département de Géologie, Niamey, Niger; ²Laboratoire de Géoressources, Géoenvironnement et Génie Civil (L3G), Département de Géologie, Faculté des Sciences et Techniques, Université Cadi Ayyad, Marrakech, Morocco and ³Argiles, Géochimie et Environnements Sédimentaires (AGEs), Département de Géologie, Quartier Agora, Université de Liège, Liège, Belgium

Abstract

This study examines the origin and distribution of clay minerals of the pedological horizons of Kori Ouallam watershed (south-western Niger). It is based on field sampling campaigns and a series of laboratory analyses. A total of 49 samples were analysed, 28 from surface horizons (0–10 cm depth) and 21 from pedological profiles (0–1 m depth). The samples were analysed by X-ray diffraction on bulk and clay (<2 µm) fractions, X-ray fluorescence spectrometry, laser granulometry, organic matter and calcium carbonate content, macroscopic observations (binocular loupe) and scanning electron microscopy equipped with an energy-dispersive spectrometry system. The pedological horizons are characterized by low organic matter contents (<1%) and no calcium carbonate. The particle-size distribution shows net textural differentiation, with a predominance of sandy loam to sandy clay loam textures in the upper horizons and clay loam to clay in the deep horizons. The main major oxides were SiO₂ (46.3–89.0%), Al₂O₃ (5.0–24.2%) and Fe₂O₃ (1.0–27.9%). Kaolinite (64–98%) is the predominant clay mineral at all horizons, associated with low to moderate proportions of illite (1–34%) and traces of chlorite. Kaolinite is essentially inherited from the parent rock, whereas illite results from chemical alteration by bisialitization of the primary minerals initially rich in potassium feldspar contained in the parent rock. However, soil texture and organic matter vary independently with clay mineralogy. An extended study of all of the pedological facies that make up south-western Niger, combined with supplementary analyses, would further improve our understanding of clay mineralogy in the Sahelian zone.

Keywords: Clay minerals, pedological horizons, Sahel, south-western Niger, X-ray diffraction

(Received 11 January 2024; revised 17 July 2024; Editor: George Christidis)

Clay minerals play a major role in the functioning of soils and in defining surface and subsurface processes (Dixon, 1991; Saffer *et al.*, 2001; Hartemink & Bockheim, 2013; Kasanin-Grubin, 2013). Soils containing smectite, for example, are more prone to water erosion than soils containing kaolinite (Wakindiki & Ben-Hur, 2002). The study of clay minerals in weathering environments during soil formation is a complicated subject due to the many parameters involved in the processes (Velde & Meunier, 2008; Ferrell *et al.*, 2013; Munroe *et al.*, 2021). In semi-arid climates, characterized by incomplete hydrolysis products of primary minerals (Curtis, 1990), different factors control soil phyllosilicate mineralogy, including erosion processes, pH and major oxide contents (in particular SiO₂, Al₂O₃, Fe₂O₃, MgO and K₂O), land use, topography, type and amount of organic matter entering the soil and soil structure and texture (Chorom *et al.*, 1994; Haynes & Naidu, 1998; Ben-Hur & Wakindiki, 2004; Kasanin-Grubin, 2013; Barré *et al.*, 2014). The distribution of clay minerals in the horizons of pedological profiles constitutes a reliable tool for determining the conditions of their formation (Singer, 1980; Eberl *et al.*, 1984; Ducloux *et al.*, 1998).

Recent work on the genesis of clay minerals in the pedological formations of semi-arid regions has demonstrated significant

progress in several regions of the world such as Morocco (Daoudi, 1996; Daoudi *et al.*, 2010; Omdi *et al.*, 2018; Gourfi *et al.*, 2020), northern Cameroon (Nguetnkam *et al.*, 2008), southern Iran (Khormali & Abtahi, 2003), and California (McFadden *et al.*, 1986). The conclusions of the abovementioned works improve our understanding of the processes linked to the mineralogy of clays in semi-arid zones. However, in the Sahel in Africa, due to the accelerated degradation of ecosystems induced by strong climatic variations and increasing human activities, research projects are largely oriented in favour of the sustainable management of natural resources and ecosystems (Lebel *et al.*, 2009; Elagib *et al.*, 2021), and few studies have focused on the genesis and evolution of clay minerals in this area. In south-western Niger, studies spanning several decades have focused on the clay assemblages of Quaternary formations (Gavaud, 1968; Bui & Wilding, 1988; Guero, 1989, 2000; Ducloux *et al.*, 1994, 1998, 2002). The hypotheses put forward concerning the genesis of clay minerals in soils are sometimes controversial and are still under discussion. This study is part of this perspective, and its main objective is to determine the origin and distribution of clay minerals in the pedological horizons of the Kori Ouallam watershed. This basin is a vast territory in south-western Niger, chosen because of the diversity of the pedological facies present, which evolved in a contrasting semi-arid climatic context. The specific objectives are: (1) to identify the different clay minerals formed at the scale of the Kori Ouallam watershed; (2) to determine the distribution pattern

Corresponding author: Salifou Noma Adamou; Email: salifounoma2000@gmail.com

Cite this article: Noma Adamou S, Daoudi L, Abdourhamane Touré A, Fagel N. Origin and distribution of clay minerals in semi-arid Sahelian soils: case of Kori Ouallam watershed, south-western Niger. *Clay Minerals*. <https://doi.org/10.1180/clm.2024.21>

of clay minerals at the scale of the pedological horizons; and (3) to critically examine the origins of the clay minerals.

Materials and methods

Study area

The study was conducted in the Kori Ouallam watershed, a semi-arid area in the extreme south-western part of Niger located between 14°4'27"N and 2°5'99"E (Fig. 1). For several decades, this vast area (10 740 km²) has been subjected to degradation of its ecosystems induced both by the hostility of the climate and the growing anthropogenic pressure on natural resources (Mamadou *et al.*, 2015; Mamoudou, 2018). The climate is of Sahelian type, characterized by a dry season from October to May and a wet winter season from June to September. The average annual rainfall ranges from ~376 mm in the north to ~516 mm in the south (DMN, 2015). This irregular but highly intensive rainfall pattern (Panagos *et al.*, 2017) falls on encrusted soils with low retention capacity (Malam Issa *et al.*, 2011; Malam-Abdou *et al.*, 2016), thereby drastically accelerating water erosion, generating an annual average potential soil loss of 1.54 t ha⁻¹ at the scale of the Kori Ouallam watershed (Noma Adamou *et al.*, 2022). Daily maximum temperatures reach 45°C in April and May, and minima of 12°C are observed between December and January. The average monthly potential

evapotranspiration is ~170 mm (DMN, 2015). The wind has a seasonal regime typical of Sahelian environments; it is characterized by two wind types: the Harmattan, a dry wind blowing from November to March in a north-east to south-west direction; and the monsoon, a wet wind blowing from south-west to north-east between May and September. The average daily wind speed usually exceeds 5 m s⁻¹ (Abdourhamane Touré *et al.*, 2011).

Geologically, the Kori Ouallam watershed is dominated by Quaternary formations (61%), consisting mainly of aeolian sandy deposits and alluvium located in the valleys at a low altitude of ~215 m (Fig. 1). The sandstone plateaus and slopes (38% of the Continental Terminal, CT3) of Middle Eocene to Quaternary age occupy the relatively high plateaus and slopes with an altitude of 374 m (Pougnnet & Greigert, 1965; Lang *et al.*, 1990). The basement of Birimian age is weakly represented and appears in the extreme north-west, occupying only 1% of the total surface area of the watershed. The woody vegetation is sparse, consisting mainly of *Guiera senegalensis*, *Combretum micranthum* and *Combretum glutinosum*, which grow on sandy and nutrient-poor soils (Ambouta & Dan Lamso, 1996; Boubacar, 2016).

Sampling protocol

The sampling protocol adopted for this study is based on the pedological map of south-western Niger (Fig. 2), which was

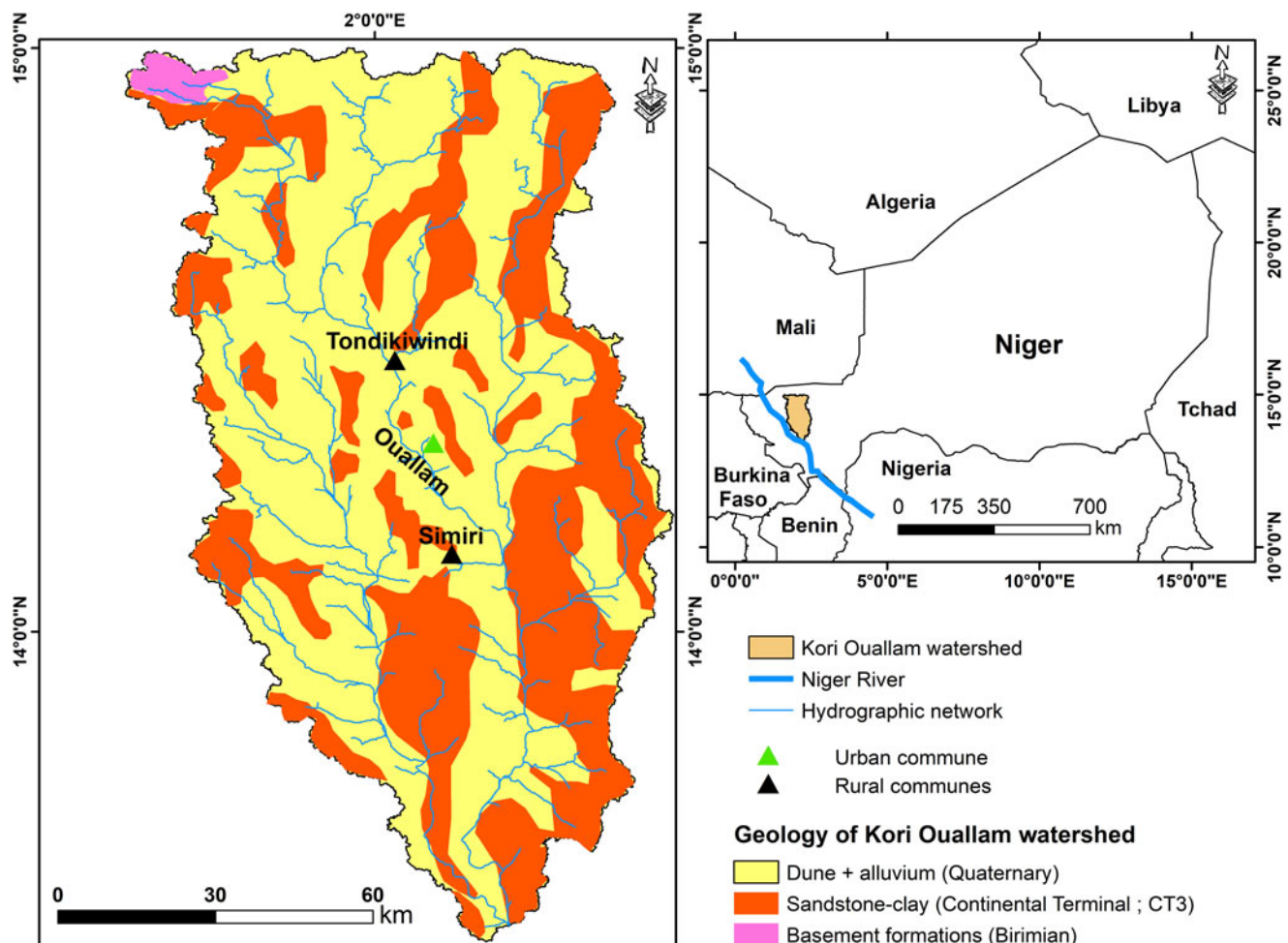


Figure 1. Location and geological map of the Kori Ouallam watershed.

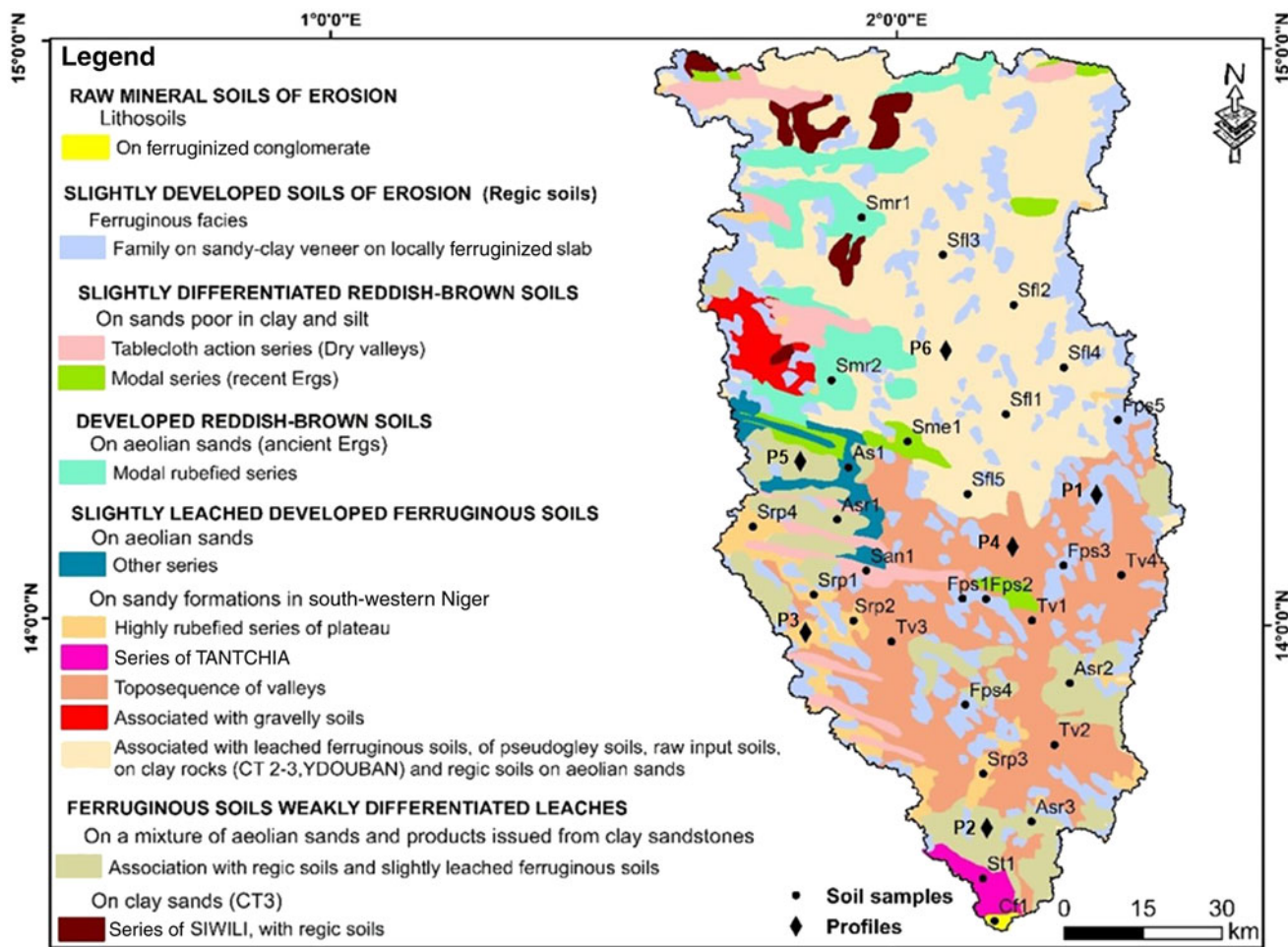


Figure 2. Pedological map of the study area and locations of the soil and profile samples (modified from Gavaud & Boulet, 1967).

drawn up on the basis of the physicochemical and geomorphological properties of the soils, with a classic nomenclature organized into soil subsets, divided into facies, families and series (Gavaud & Boulet, 1967). The diversity and extent of the pedological formations, combined with the recurrent security threats in the far north of the Kori Ouallam watershed, meant that the investigation was focused on the major subsets of the soil types representing the most dominant facies (Fig. 2). A total of 49 samples, divided into two groups, were obtained from the entire watershed. The first group consisted of 28 soil samples from the upper soil horizons between 0 and 10 cm in depth, and the second group consisted of 21 profile samples from the different horizons from six 1 m-thick pedological profiles (Figs 2 & 3; Ducloux *et al.*, 2002). The sampled pedological units are characterized by geomorphological, geological and environmental diversity (Fig. 4). The Munsell colour code was used to identify the colour of the horizons of the various profiles.

Methods of analysis

The samples were subjected to a series of laboratory analyses for characterization of their mineralogical, physicochemical and microscopic properties. These included X-ray diffraction (XRD), particle-size distribution, soil organic matter and calcium

carbonate content and X-ray fluorescence (XRF) spectrometry analyses and microscopic observations using a binocular magnifying lens and a scanning electron microscope (SEM) equipped with an energy-dispersive X-ray spectroscopy (EDX) system.

The mineralogical composition was determined by XRD using a Bruker D8-Eco Advance diffractometer with monochromatic Cu-K α radiation (scanning step size: 0.02°; time step: 0.6 s) operated at 40 kV and 25 mA from 2 to 70°2 θ on powdered bulk sediment and on the <2 μ m fraction (Argiles, Géochimie et Environnements Sédimentaires (AGEs), Department of Geology, University of Liège). The bulk mineralogy was identified on samples gently crushed and passed through a 250 μ m dry sieve. The <2 μ m clay fraction samples were prepared according to the standard procedure – namely, with separation by settling in a water column and then mounting as oriented aggregates on glass slides (Moore & Reynolds, 1997). For each sample, three XRD traces were recorded: air dried (N), ethylene glycol solvated for 24 h (EG) and heated at 500°C for 4 h (H). The background noise of the XRD traces was removed and the line position, intensity peak and integrated area were calculated using *HighScore Plus* software. Semi-quantitative estimates of the minerals present were achieved by measuring the intensity of the diagnostic peaks of the various minerals identified by XRD and application of correction factors specific to each mineral for the bulk samples and the EG

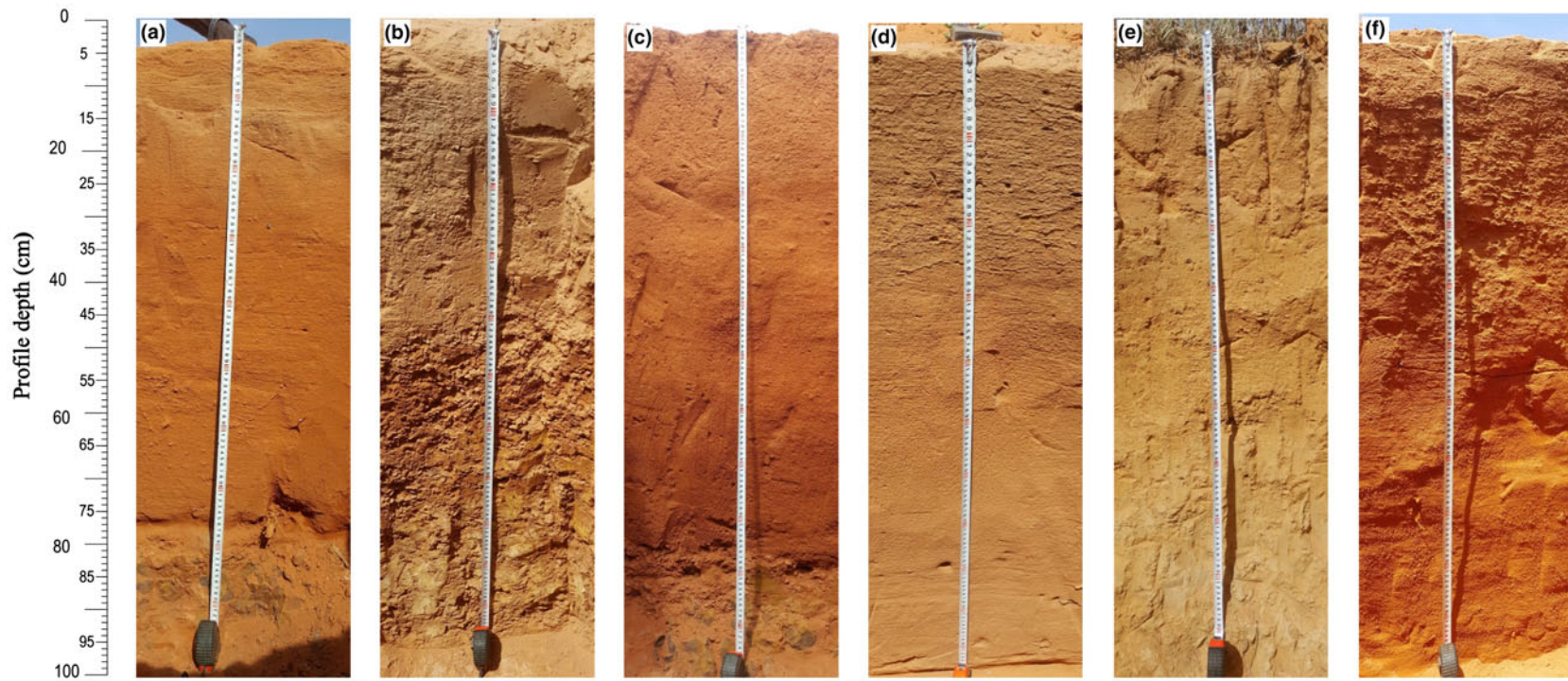


Figure 3. Pedological profiles: (a) profile 1, (b) profile 2, (c) profile 3, (d) profile 4, (e) profile 5 and (f) profile 6.

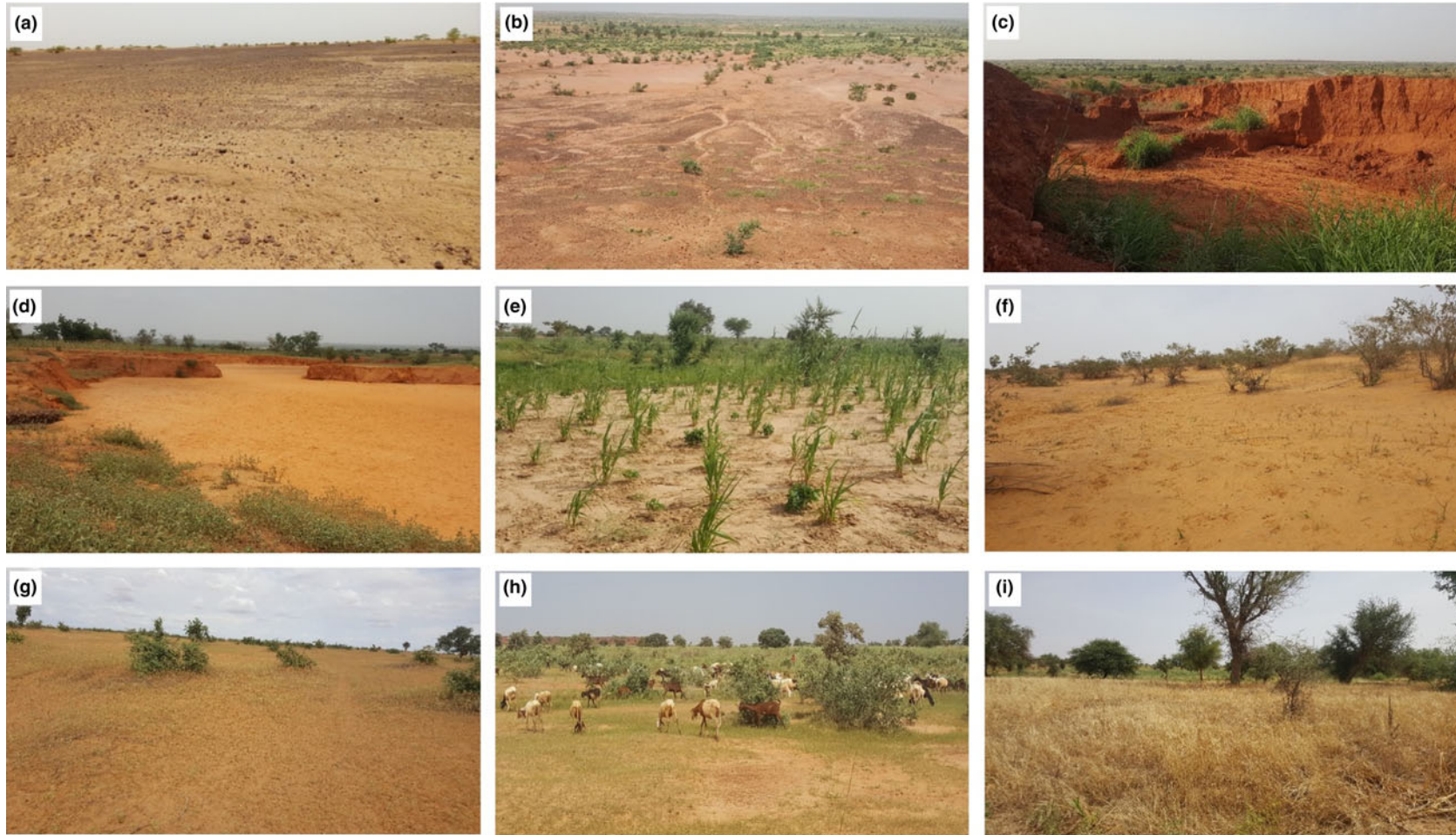


Figure 4. Sampled landscapes: (a) lateritic soils of low-slope plateaus of the Continental Terminal, (b) lateritic soils of the steep versants of the Continental Terminal, (c) Continental Terminal soils from bank erosion, (d) sandy deposits of the valleys from rainwater drainage, (e) low-slope agricultural Quaternary lands, (f) encrusted soils of the Quaternary glaciais, (g) fallow lands, (h) pastoral lands and (i) set-aside lands.

Table 1. Semi-quantitative method for the estimation of sample mineralogical composition.

Sample type	Minerals	Diagnostic peak (Å)	Correction factor	Reference
Powder	Quartz	3.37–3.31	1.00	Cook <i>et al.</i> (1975)
	Hematite	2.71–2.68	3.33	
	Goethite	2.46–2.43	7.00	
	Plagioclase	3.21–3.16	2.80	
	K-feldspar	3.26–3.21	4.30	
Clay	Total clay	4.47	20.00	Boski <i>et al.</i> (1998) Fagel <i>et al.</i> (2003)
	Kaolinite (EG)	7.20–7.10	0.70	
	Illite (EG)	10.00	1.00	

series from the clay fractions following the methodology described in Table 1.

The particle-size analyses were carried out using a HORIBA LA-300 laser diffraction analyser to determine the clay, silt and sand particles with a monochromatic laser beam (Baosupee *et al.*, 2014). The total organic matter content was determined from loss on ignition (LOI) at 550°C for 4 h (Heiri *et al.*, 2001). Calcium carbonate content was determined with the calcimeter method that uses 10% HCl to measure the volume of carbon dioxide (CO₂) released (Hulseman, 1966; Muller & Gatsner, 1971). The abovementioned analyses were carried out at the Laboratory of Georesources, Geoenvironment and Civil Engineering (L3G), Cadi Ayyad University, Marrakech.

SEM observations were also carried out using a Tescan Vega-3 SEM equipped with a high-performance EDX system at the Analysis and Characterisation Centre (CAC), Cadi Ayyad University, Marrakech.

Results

Soil samples

Particle-size distribution and organic matter and calcium carbonate content

The soils of the Kori Ouallam watershed are characterized by low organic matter content (<1%; Table 2). No trace of calcium carbonate (CaCO₃) was detected in any sample. Laser granulometry allowed the identification of seven classes of soil textures, marked by a predominance of sandy clay loam and sandy loam textures (Fig. 5 & Table 2).

Mineralogical composition

The semi-quantitative analysis of the soil samples by XRD shows that, at the scale of the whole watershed and independently of the pedological facies, the mineralogical composition of the bulk samples is constant. The samples are dominated by quartz (60–96%), associated with total clay (2–29%), K-feldspar (0–5%), plagioclase (0–4%) and hematite (0–3%; Figs 6a & 7a). The highest proportions of total clay were observed on lateritic soils (Fps3, Fps4, Fps5) formed on the sandstones. This lithology is especially observed on the plateaus and versants of the Continental Terminal (Fig. 2).

The mineralogical composition of the clay fractions does not show a variable spatial trend. Kaolinite is the most abundant clay mineral (82–99%), associated with illite (1–18%, average 4%), whilst chlorite is present in trace amounts (Figs 6b & 7b).

Chemical composition

The chemical composition of the soil samples consists mainly of SiO₂ (70–89%), Al₂O₃ (5–20%), Fe₂O₃ (1–4%) and P₂O₅ (~2%). MgO, K₂O, MnO, Na₂O and TiO₂ are present in low

Table 2. Results regarding the particle-size distribution and organic matter content of the soils.

Samples	Lithology	Organic matter (%)	Particle size (%)			Texture
			Clay (<2 µm)	Silt (2–50 µm)	Sand (>50 µm)	
Sfl1	Quaternary formations	0.62	27	24	49	Sandy clay loam
Sfl2	Quaternary formations	0.15	42	16	42	Clay
Sfl3	Quaternary formations	0.16	6	3	91	Sand
Sfl4	Quaternary formations	0.19	11	5	84	Loamy sand
Sfl5	Quaternary formations	0.27	18	10	72	Sandy loam
Tv1	Sandstone–clay	0.19	47	28	25	Clay
Tv2	Quaternary formations	0.16	30	25	45	Clay loam
Tv3	Quaternary formations	0.23	32	20	48	Sandy clay loam
Tv4	Quaternary formations	0.20	17	11	72	Sandy loam
Fps1	Sandstone–clay	0.20	20	11	69	Sandy clay loam
Fps2	Sandstone–clay	0.30	8	3	89	Loamy sand
Fps3	Sandstone–clay	0.44	25	34	41	Loam
Fps4	Sandstone–clay	0.62	22	18	60	Sandy clay loam
Fps5	Sandstone–clay	0.32	19	22	59	Sandy loam
Srp1	Sandstone–clay	0.18	35	20	45	Clay loam
Srp2	Quaternary formations	0.29	34	24	42	Clay loam
Srp3	Quaternary formations	0.08	12	15	73	Sandy loam
Srp4	Sandstone–clay	0.14	30	18	52	Sandy clay loam
Asr1	Quaternary formations	0.26	11	12	77	Sandy loam
Asr2	Sandstone–clay	0.15	16	19	65	Sandy loam
Asr3	Sandstone–clay	0.36	31	10	59	Sandy clay loam
Smr1	Quaternary formations	0.15	9	2	89	Loamy sand
Smr2	Quaternary formations	0.18	15	3	82	Sandy loam
Sme1	Quaternary formations	0.21	8	7	85	Loamy sand
San1	Quaternary formations	0.10	22	12	66	Sandy clay loam
As1	Sandstone–clay	0.27	15	9	76	Sandy loam
St1	Quaternary formations	0.17	27	9	64	Sandy clay loam
Cf1	Sandstone–clay	0.16	11	5	84	Loamy sand

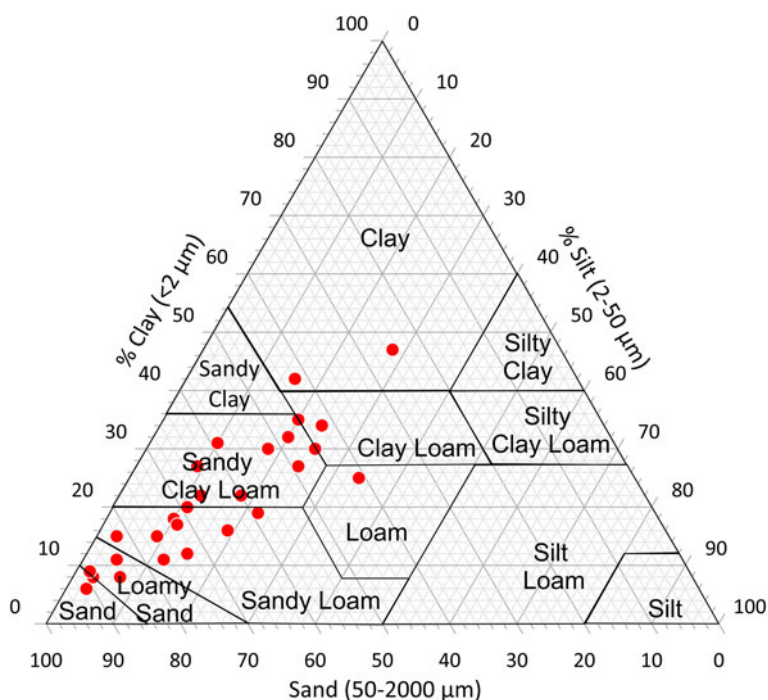


Figure 5. Texture classes of the soil samples.

concentrations, sometimes below the detection limit of the analytical method (Table 3). CaO is below the detection limit for all of the samples. Al₂O₃ and Fe₂O₃ are more abundant in samples Fps3, Fps4 and Fps5 (13–20 and 3–4 wt.%, respectively), associated with the lowest contents of SiO₂ (70–78 wt.%). The abundances of SiO₂, Al₂O₃ and Fe₂O₃ are in accord with the mineralogical composition dominated by quartz, K-feldspar, clay minerals and hematite. Values below the detection limit for

Table 3. Major chemical composition of oxides (wt.%) in the soil samples.

Sample	SiO ₂	Al ₂ O ₃	Fe ₂ O ₃	MgO	K ₂ O	Na ₂ O	TiO ₂	P ₂ O ₅	LOI (950°C)
Sfl1	73.1	18.7	3.0	0.5	0.4	<DL	1.2	2.2	0.8
Sfl2	80.6	11.9	1.5	2.1	0.3	0.2	0.6	2.4	0.4
Sfl3	79.7	12.3	1.9	1.7	0.4	0.9	0.5	2.4	0.3
Sfl4	85.7	6.4	1.4	2.2	0.2	1.2	0.4	2.2	0.3
Sfl5	84.9	8.8	1.3	1.0	0.4	0.4	0.6	2.4	0.2
Tv1	83.0	10.8	1.7	0.3	0.4	<DL	0.7	2.6	0.5
Tv2	88.3	7.1	0.9	<DL	0.3	0.3	0.6	2.2	0.2
Tv3	79.1	12.4	3.6	0.5	0.5	<DL	0.9	2.1	0.7
Tv4	86.7	7.1	2.1	0.3	0.3	0.2	0.5	2.3	0.4
Fps1	84.1	10.1	1.3	0.5	0.3	0.7	0.5	2.2	0.4
Fps2	81.7	11.6	1.8	0.9	0.5	<DL	0.6	2.5	0.5
Fps3	78.2	13.4	3.7	0.3	0.5	<DL	1.1	2.3	0.6
Fps4	72.3	17.7	4.2	0.8	0.4	<DL	1.3	2.4	1.1
Fps5	70.2	20.2	3.6	0.6	0.5	<DL	1.4	2.4	1.3
Srp1	80.8	10.7	2.5	2.3	0.3	<DL	0.8	2.2	0.4
Srp2	81.6	12.7	1.8	0.1	0.2	<DL	0.7	2.6	0.3
Srp3	88.3	5.7	1.3	1.1	0.3	0.1	0.5	2.3	0.4
Srp4	87.4	7.3	1.1	0.5	0.3	0.3	0.6	2.4	0.2
Asr1	87.6	7.4	1.5	0.3	0.4	<DL	0.5	2.1	0.3
Asr2	89.5	5.3	1.4	0.5	0.3	<DL	0.7	2.3	0.2
Asr3	84.9	9.5	1.6	0.4	0.3	0.2	0.5	2.5	0.2
Smr1	82.0	12.1	1.9	<DL	0.4	0.5	0.6	2.5	0.1
Smr2	82.2	12.1	1.5	0.5	0.2	0.1	0.5	2.7	0.2
Sme1	86.3	7.3	2.5	0.3	0.4	0.1	0.5	2.2	0.5
San1	89.6	6.0	0.8	0.4	0.3	<DL	0.4	2.2	0.3
As1	87.6	6.8	1.8	0.3	0.3	<DL	0.5	2.5	0.3
St1	84.6	9.1	1.7	0.4	0.3	0.5	0.6	2.5	0.3
Cf1	88.5	5.7	1.0	0.1	0.3	1.0	0.7	2.4	0.3

<DL= below detection limit.

CaO can be explained by the absence of carbonate minerals and the low abundance of plagioclase.

Profile samples

Physicochemical and mineralogical characteristics

The textures of the samples from the pedological profiles range from sandy loam to sandy clay loam in horizons A and B (Fig. 8a,b) and from clay loam to clay in horizon C and the parent rock (Fig. 8c,d). The samples are characterized by a low organic matter content (<1%) and are free of calcium carbonate (Fig. 9). The particle-size distribution shows an increase in clay and silt particles with depth at the expense of sand particles (Fig. 9).

Quartz is the most abundant phase in the various horizons (23–95%), associated with total clay (3–45%), hematite (0–16%), goethite (0–15%), K-feldspar (0–14%) and traces of anatase (<1%). In some samples, the presence of minerals with a high iron content (hematite, goethite) is also supported by the geochemical analyses, showing high proportions of Fe₂O₃ ranging from 5% to 28% (Table 4). These minerals were identified mainly in the parent rock (P1, P2 and P3; Fig. 9). The total clay content increases at depth, from 3% in the subsurface to 45% in horizon C or the parent rock. Abundant K-feldspar (10–14%) is detected exclusively in the parent rock (profiles P1, P2 and P4), decreasing progressively or abruptly upwards.

The mineralogical composition of the clay fractions is similar to the soil composition, marked by the dominance of kaolinite (64–98%). Illite is present in variable concentrations (0–34%), with a maximum being recorded in the upper horizons of profiles P1, P2 and P4. Chlorite was detected in trace amounts in all samples (<1%).

Microscopic analysis

The SEM analysis was carried out on samples collected from the various soil horizons. The minerals are difficult to identify from

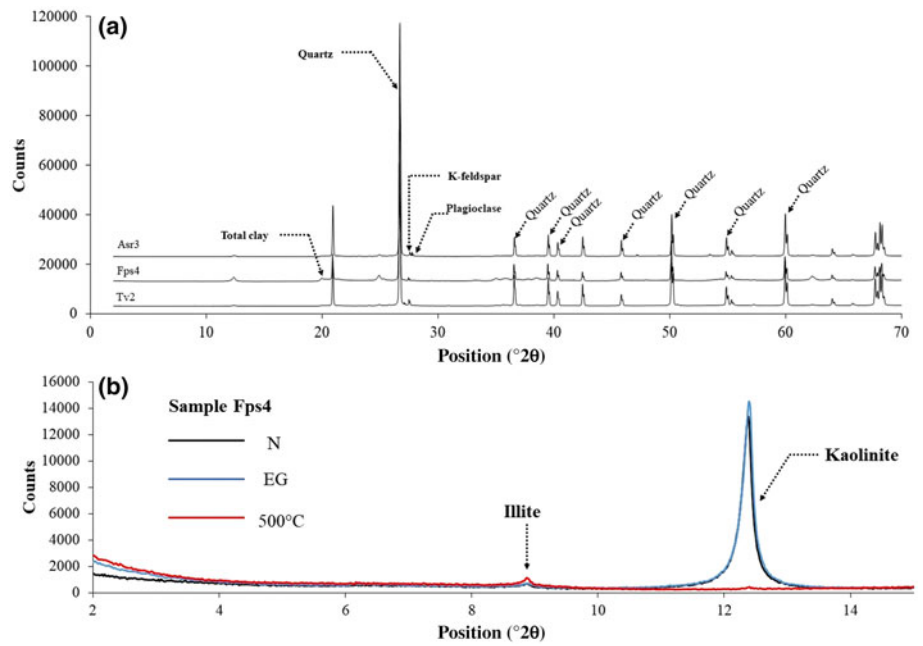


Figure 6. XRD traces of (a) bulk samples and (b) clay fractions (N, EG, 500°C).

their shape (Fig. 10a). EDX microanalysis (Fig. 10b) allowed identification of kaolinite ($0.7 < \text{Si}/\text{Al} < 2.2$). The particles of kaolinite are characterized by an average Fe_2O_3 content estimated at 2.41% (Fig. 10b), which is typical of tropical soils (Herbillon *et al.*, 1976).

Discussion

Grain-size distribution

The grain-size distribution shows a textural differentiation between the different horizons of the same profile that is marked

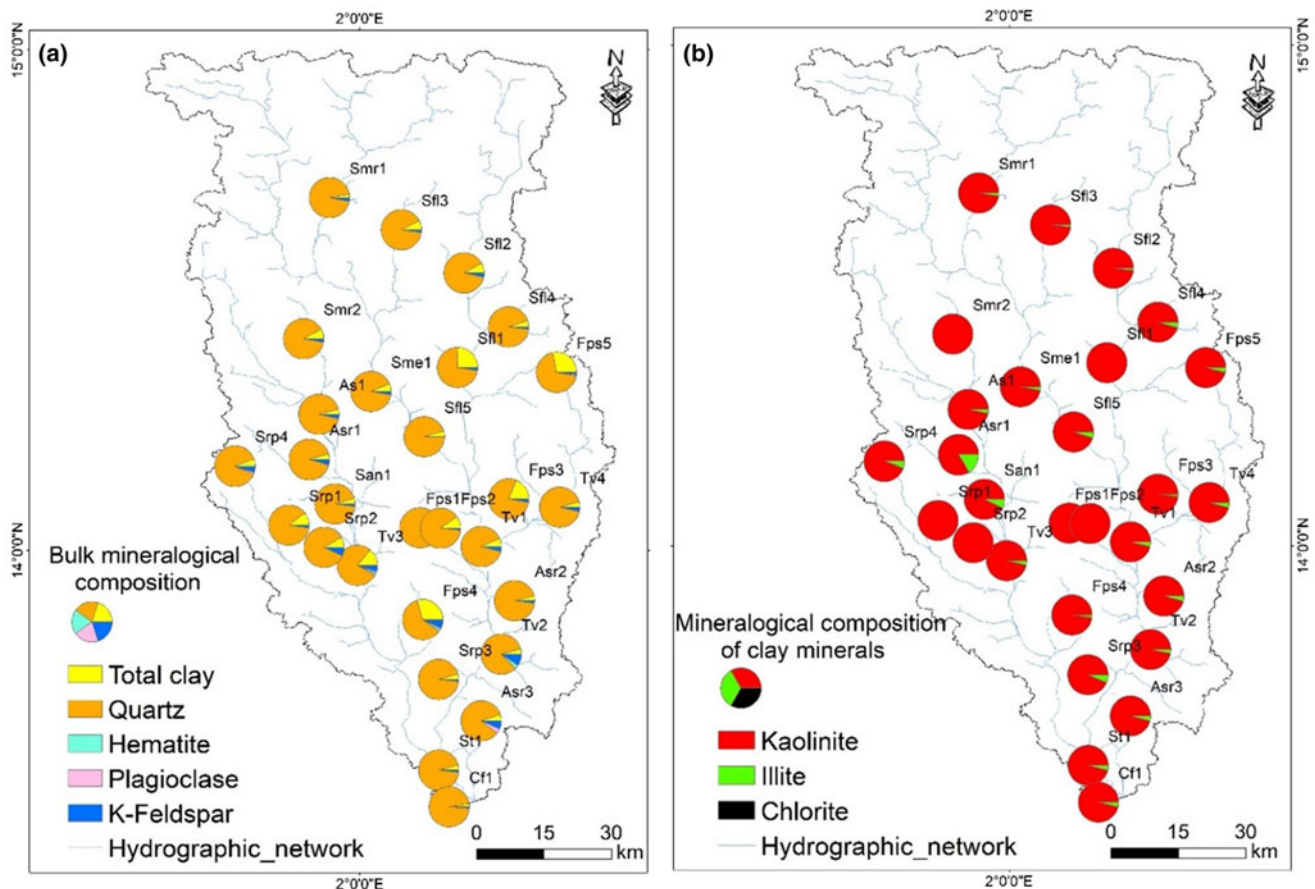


Figure 7. Mineralogical composition of soils: (a) bulk mineralogy and (b) clay mineralogy.

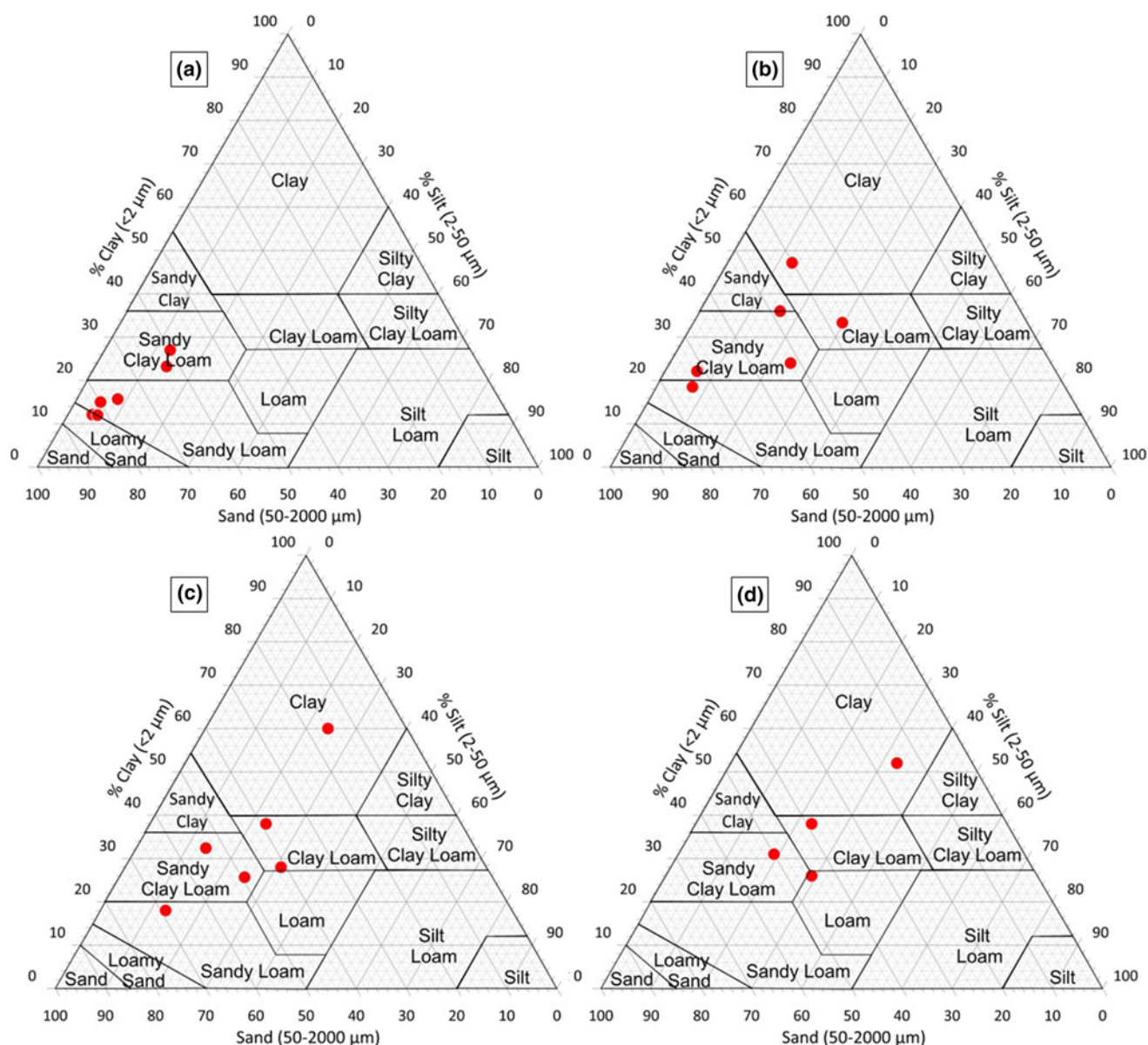


Figure 8. Texture classes of profile horizons: (a) horizon A, (b) horizon B, (c) horizon C and (d) parent rock.

by a predominance of sandy fractions in the surface horizons (Fig. 9). This distribution pattern of granulometric fractions is consistent with previous work carried out in south-western Niger in the villages of Sona and Tillakaina, where 11 out of 15 profiles showed a similar trend (Ducloux *et al.*, 2002). In the Sahel, this textural differentiation is attributable, on the one hand, to the intense mechanical material transfer processes induced by runoff (Descroix *et al.*, 2009; Mamadou *et al.*, 2015) and, on the other hand, to active aeolian processes acting on a surface with low roughness (Pierre *et al.*, 2014; Abdourhamane Touré *et al.*, 2019). In the Sahelian climatic context, Guero (2000) and Ducloux *et al.* (1998, 2002) highlighted another process underlying the origins of the particle-size distribution at the scale of the pedological profiles: the phenomenon of ‘xerolysis’, which is a mechanism resulting from the alteration and/or dissolution of the clay particles at the soil surface within a relatively hot climate.

Origin and distribution of non-clay minerals

Soils from the upper horizons of the pedological profiles have high organic matter contents due to the accumulation of organic components and plant debris. In contrast, the soils prospected in the Kori Ouallam watershed present insignificant organic matter contents (~1%; Fig. 9). Furthermore, the organic matter content of soils is not related to the mineralogical composition of clays. Similar results have been recorded on soils sampled across south-western Niger (Fofana *et al.*, 2008; Obame *et al.*, 2014). This organic matter deficit in soils is specific to Sahelian semi-arid environments (FAO, 2014; Suzuki *et al.*, 2014, 2016).

The samples analysed are free of calcium carbonate (CaCO_3), in accordance with the low CaO concentrations (below the detection limit) obtained by XRF fluorescence (Tables 3 & 4) and the notable absence of carbonate minerals such as calcite, aragonite and dolomite in the mineralogical composition (Figs 6, 7 & 9).

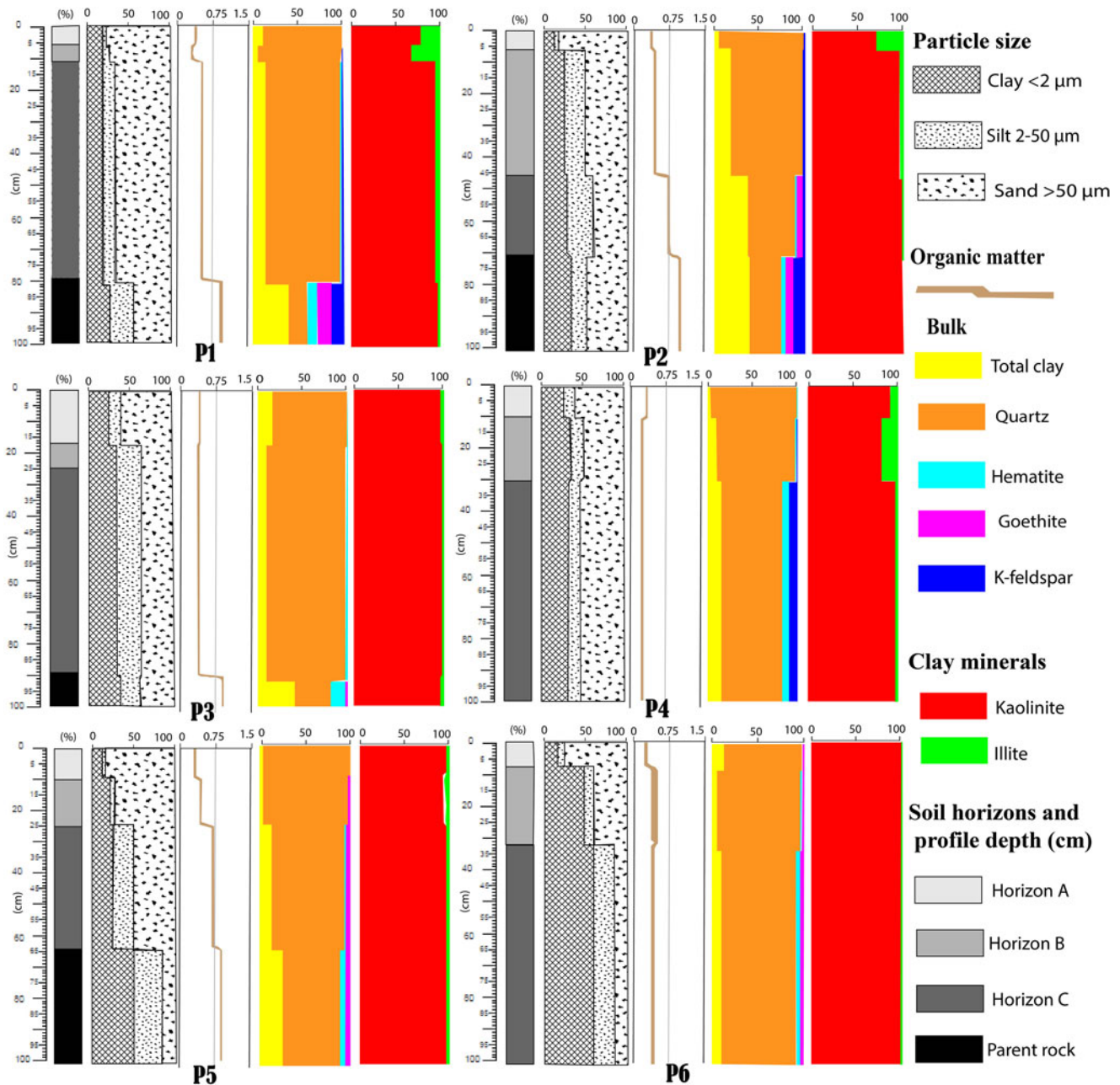


Figure 9. Physicochemical and mineralogical properties of the soil profile samples: profile 1 (P1), profile 2 (P2), profile 3 (P3), profile 4 (P4), profile 5 (P5) and profile 6 (P6).

This deficit in carbonate minerals has also been observed in the Middle Niger Valley (Guero, 1989) and is largely attributed to an absence of calcareous sources in the parent materials.

Quartz is the most abundant phase in all of the analysed samples. Its content varies from 60% to 96% in surface samples and from 23% to 95% through the profiles. Observation under the binocular lens shows that the quartz grains of the samples from all soil horizons are angular, suggesting that the quartz grains in the soils were most probably inherited from the underlying parent rock rather than from aeolian supplies.

The decreasing iron oxide contents (hematite, goethite) upwards from the deep horizons to the surface horizons has also been observed in the Niger River valley (Guero, 1989). This trend of iron enrichment in lateritic processes resulting

from alteration of the parent rock is characteristic of intertropical areas such as the Kori Ouallam watershed (Negrão & da Costa, 2021).

Origin and distribution of clay minerals

The processes of clay mineral genesis and evolution in soils of semi-arid areas have generated a wide variety of sometimes controversial discussion (Khormali & Abtahi, 2003; Wang *et al.*, 2013; Zhang & Guo, 2014; Omdi *et al.*, 2018; Gourfi *et al.*, 2020). In this section, we will critically examine the different processes that may be at the origin of the formation of the clay minerals identified in the various pedological horizons of the Kori Ouallam watershed.

Table 4. Major chemical composition of oxides (wt.%) in the profile samples.

Profile	Horizon	Munsell soil colour	SiO ₂	Al ₂ O ₃	Fe ₂ O ₃	MgO	K ₂ O	Na ₂ O	TiO ₂	P ₂ O ₅	LOI (950°C)
P1	P1A	Red (2.5YR 5/6)	83.9	9.2	1.8	1.1	0.3	0.5	0.7	2.3	0.2
	P1B	Reddish brown (2.5YR 5/4)	85.6	8.5	1.9	<DL	0.3	0.4	0.6	2.4	0.3
	P1C	Red (2.5YR 4/6)	80.2	13.2	2.1	0.5	0.3	<DL	0.8	2.4	0.3
	P1PR	Dusky red (10R 3/3)	46.3	23.6	21.0	3.5	<DL	0.9	1.2	2.2	1.2
P2	P2A	Light reddish brown (2.5YR 6/3)	85.7	9.6	1.1	0.3	0.3	<DL	0.6	2.3	0.2
	P2B	Reddish brown (5YR 5/4)	76.1	16.1	2.5	0.6	0.3	0.1	1.1	2.5	0.7
	P2C	Red (2.5YR 5/6)	60.0	24.2	8.6	1.6	0.2	0.6	1.2	2.2	1.4
	P2PR	Reddish yellow (7.5YR 7/6)	65.1	22.4	5.9	1.2	0.1	0.7	1.2	2.2	1.2
P3	P3A	Red (10R 4/6)	75.3	16.1	4.3	<DL	0.4	<DL	0.8	2.5	0.6
	P3B/C	Red (10R 4/8)	77.6	13.1	3.5	1.3	0.3	0.3	0.8	2.6	0.6
	P3PR	Dark yellowish brown (10YR 4/6)	47.1	16.7	27.9	2.9	0.1	1.0	0.5	2.1	1.6
P4	P4A	Brown (10YR 5/3)	83.9	9.9	1.6	0.4	0.4	0.5	0.5	2.3	0.5
	P4B	Red (2.5YR 4/6)	83.9	10.0	1.6	0.5	0.3	0.3	0.5	2.5	0.5
	P4C	Reddish yellow (7.5YR 6/6)	80.8	10.3	1.7	3.2	0.3	<DL	0.6	2.6	0.5
P5	P5A	Light reddish brown (5YR 6/4)	88.0	6.6	1.6	0.2	0.3	<DL	0.6	2.4	0.3
	P5B	Pink (5YR 7/4)	81.8	11.1	1.4	1.7	0.2	0.5	0.4	2.6	0.3
	P5C	Reddish yellow (7.5YR 6/6)	73.9	17.6	3.3	1.0	0.2	<DL	0.8	2.6	0.6
	P5PR	Yellow (10YR 7/6)	68.6	21.1	5.0	0.5	0.2	0.1	1.1	2.4	1.0
P6	P6A	Reddish brown (2.5YR 5/3)	82.7	11.6	1.3	0.3	0.4	<DL	0.6	2.4	0.6
	P6B	Reddish brown (2.5YR 5/4)	83.8	10.6	0.8	1.2	0.3	0.1	0.6	2.2	0.3
	P6C	Yellowish red (5YR 5/6)	77.9	16.2	1.3	0.5	0.4	0.1	0.7	2.4	0.6

<DL= below detection limit.

Kaolinite

The clay minerals identified are dominated by kaolinite in all horizons, regardless of the diversity of pedological facies or topography. The predominance of kaolinite in the pedological formations of south-western Niger has been well documented in several previous works (Bui & Wilding, 1988; Ducloux *et al.*, 1994, 1998, 2002; Guero, 2000). Kaolinite represents the main clay mineral in tropical Sahelian soils (Lang *et al.*, 1990; Driessen *et al.*, 2001; Traoré *et al.*, 2007; Journet *et al.*, 2014), which might partly explain the low reactivity and productivity of these soils (Duchaufour, 1982; Saffer *et al.*, 2001). In all six soil profiles surveyed in the Kori Ouallam watershed, kaolinite abundance remained constant with depth (Fig. 9), which might be largely due to its presence in the parent rocks, as observed in similar semi-arid environments, notably in south-western Niger (Guero, 1989; Ducloux *et al.*, 2002), in central-western Morocco (Omdi *et al.*, 2018; Gourfi *et al.*, 2020) and in southern Iran (Khorrami & Abtahi, 2003). The parent rocks studied are mainly composed of alluvial Quaternary formations (61%; Fig. 1) rich in kaolinite (Fig. 9). Those formations would constitute a very probable source of the kaolinite identified in the pedological profiles. The observed trend in kaolinite content suggests that the soil materials as a whole have not undergone significant changes. These materials seem to have evolved under a similar climate to the present one (Mohr *et al.*, 1972; Singer, 1980), whose sedimentary environment appears to be relatively constant (Bauluz *et al.*, 2014). The irregular morphology of the kaolinites observed by SEM in all of the samples (Fig. 10a) indicates that these may be of detrital origin, most often resulting from remobilization of parent materials, similar to the kaolinite in the sedimentary deposits of the Oliete Basin (north-east Spain; Bauluz *et al.*, 2008). These authors observed that kaolinites of detrital origin are characterized by a xenomorphic form that is difficult to recognize and is poorly crystallized, whereas diagenetic kaolinites

are idiomorphic, with good crystallinity, and are easily recognizable, thus highlighting their authigenic origins, with a clear variation in content depending on depth and burial conditions (Arostegui *et al.*, 2001; Daoudi *et al.*, 2010; Bauluz *et al.*, 2014). Extreme chemical alteration processes such as monosialitization linked to morphoclimatic conditions may also lead to the formation of kaolinite (Nguetnkam *et al.*, 2008). However, in the Kori Ouallam watershed (Sahelian context specific to south-western Niger), alternating hot and humid climatic conditions associated with a low relief topography slow down the processes of monosialitization. These conditions instead favour bisialitization alteration processes that yield 2:1 clay minerals (smectite or illite). The formation of kaolinite by monosialitization requires, in addition to a suitable climate, good drainage conditions controlled by a steeply sloping topography (Chamley, 1989; Righi, 1999), which is not the case for the present study. The combined analysis of the various indices suggests that in the studied soils of the Kori Ouallam watershed the kaolinite is principally inherited from the parent materials.

Illite

The proportions of illite remain low in the various types of studied soils (Fig. 7b). However, at the scale of the pedological profiles (Fig. 9), two distribution patterns are observed. The first reflects a low and stable trend all along the profiles (profiles P3, P5 and P6), and the second shows an increase in illite contents upwards (profiles P1, P2 and P4; Fig. 9). An ascending evolution of illite proportions has also been observed in some soil profiles in central-western Benin (Junge & Skowronek, 2007). Guero (1989; south-western Niger) observed a third pattern of illite content evolution in one out of six profiles, marked by relatively low proportions of illite (~5 wt.%) in the surface horizons that progressively increase at depth (up to 15 wt.%). It appears that the distribution of illite in the Sahelian pedological formations is

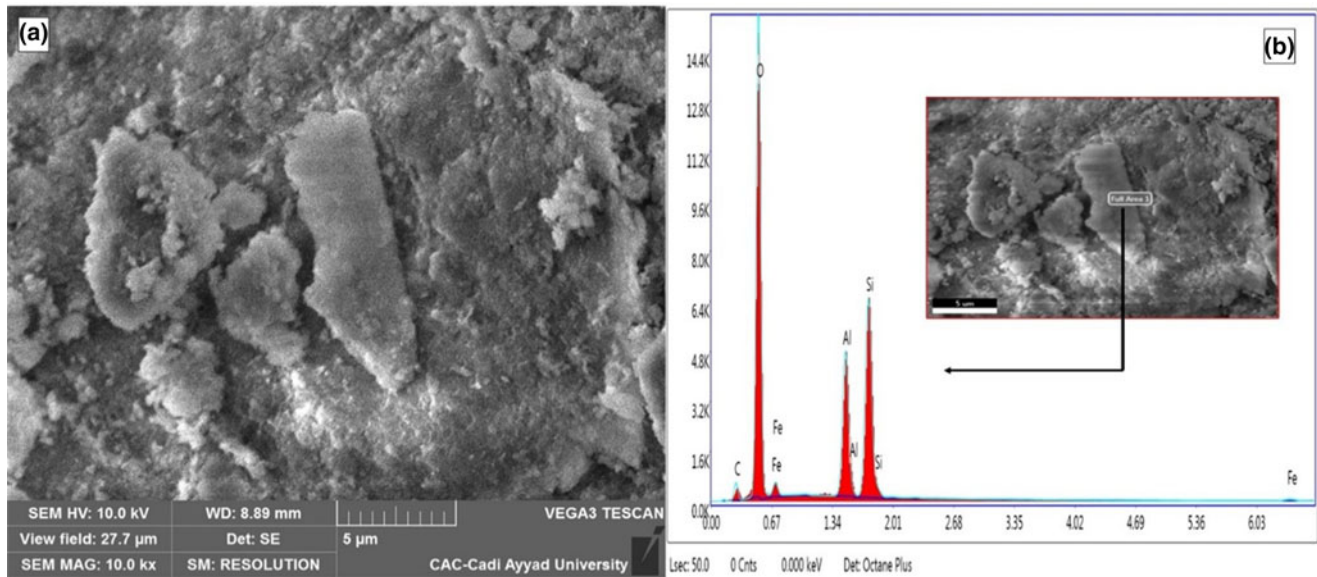


Figure 10. (a) SEM images and (b) EDX spectra of kaolinite crystals.

more complex, implying that various processes probably led to the formation of illite. In the following paragraphs, we will present and discuss the main hypotheses to determine the mechanism likely to be responsible for illite enrichment in the upper horizons of the profiles studied.

Terrigenous aeolian dust might be a source of illite at the surface horizons of south-western Niger soils (McFadden *et al.*, 1986; Møberg *et al.*, 1991; Journet *et al.*, 2014). The Sahelian region is one of the main sources of dust emission in the world (Prospero & Nees, 1986; Coudé-Gaussen, 1991; Prospero *et al.*, 2002; Bergametti *et al.*, 2017; Muhs *et al.*, 2021) through a seasonal east-west transport by the Harmattan wind from Africa to the Atlantic Ocean (McTainsh & Walker, 1982). However, the two observed patterns reject a common aeolian supply. Indeed, in the studied region, the wind affects large geographical areas due to its low relief and sparse vegetation.

Differential transport processes by water would be responsible for the enrichment of surface horizons in illite; kaolinite would be more easily transported, which would lead to an increase in the illite proportions of surface samples (Shi *et al.*, 2015; Omdi *et al.*, 2018). This hypothesis would also be unlikely to explain this mineralogical differentiation. Indeed, the processes of differential sedimentation mechanisms between illite and smectite are better understood due to the small size and flaky appearance of smectite particles (Gibbs, 1977; Omdi *et al.*, 2018). Moreover, the profiles that are impacted by this differentiation and that should be located in regions exposed to hydrodynamic processes are instead located on flat landforms, which are areas that are less exposed to water action and runoff.

As an alternative hypothesis, illite may result from incomplete hydrolysis processes by bisialitization and transformations of primary minerals from parent rocks (Singer, 1984; Jaboyedoff, 2001; Velde & Meunier, 2008). The geomorphological and climatic characteristics of south-western Niger are favourable to the partial hydrolysis responsible for the formation of illite. It appears that illite forms by alteration of K-rich primary minerals observed in the parent rock of profiles P1, P2 and P4 (10–14% K-feldspar; Fig. 9). However, in the profiles characterized by very low illite

contents (profiles P3, P5 and P6), the K-feldspar peaks were not identified on the XRD traces of the parent rock (Fig. 9). In studying the genesis of pedological clays, Pédro (1984) observed that bisialitization is one of the major processes underlying the origin of the formation of type 2:1 clays, mainly illite. Paquet (1970) analysed the geochemical evolution of clay minerals in Mediterranean and tropical climates and concluded that in tropical zones with contrasting seasons, similar to south-western Niger, chemical weathering processes are more intense in those soils with a direct involvement of surface dynamics.

In the context of this study, the illite chemistry index can provide useful information on the alteration processes and conditions of illite formation. Examination of this index, determined from the ratio of the areas of peaks at 5 and 10 Å after ethylene glycol solvation (Esquevin, 1969), shows that in the pedological formations of the Kori Ouallam watershed the illite chemistry index values range from 1.10 to 1.79 (with an average of 1.52) on soil samples, and from 0.75 to 2.20 (with an average of 1.82) on profile samples. All illite chemistry index values obtained are higher than 0.5, characteristic of Al-rich illite and indicating the prevalence of chemical weathering, in contrast to illites rich in Fe and Mg (illite chemistry index < 0.5) resulting from physical weathering (Chamley, 1989; Petschick *et al.*, 1996; Wang *et al.*, 2011). The chemical weathering process is also supported by the kaolinite/illite ratio, which is very high for all of the samples, reflecting the prevalence of hydrolysis processes operating in the soils of the Kori Ouallam watershed (Liu *et al.*, 2007).

Conclusions

This study examines the physicochemical and mineralogical characteristics and the resulting processes of the soil complexes in the Kori Ouallam watershed (south-western Niger). In this area, the soils are characterized by a deficit in nutrients, which is reflected by low organic matter contents and predominantly sandy clay loam textures, among other factors.

The clay mineralogy of the soils studied shows a classic distribution composed mainly of kaolinite and illite, which could be

attributed to two distinct origins. The first is related to the inheritance from the parent rock, an origin that essentially concerns kaolinite, as evidenced by the morphoclimatic conditions of the study area and the distribution pattern of clay assemblages, particularly at the scale of the pedological profiles.

The second origin of the clays is thought to result from chemical alteration processes by bisialitization of the primary minerals, mainly K-feldspar, present in the parent rock, which lead mainly to the formation of illite.

The pedological materials that make up the soils result from a combination of inheritance and incomplete chemical weathering of the parent rock. The results of this study might serve as a solid basis for understanding the mechanisms of clay mineral genesis and evolution in semi-arid environments, particularly the Sahel, where scientific study of clays is made highly complex due to constraints linked to the availability of means, particularly technical ones.

Financial support. Financial support was provided by the CNRST of the Kingdom of Morocco 'Domaines Prioritaires de la Recherche Scientifique et du Développement Technologique' (Ref. PPR1/2015/63), by the 'Projet de Coopération Bilatérale Belgique-Maroc ERASMUS +' and by the ANAB 'Agence Nigérienne des Allocations et des Bourses', all of which are gratefully acknowledged.

Conflicts of interest. The authors declare none.

References

- Abdourhamane Touré A., Rajot J.L., Garba Z., Marticorena B., Petit C. & Sebag D. (2011) Impact of very low crop residues cover on wind erosion in the Sahel. *Catena*, **85**, 205–214.
- Abdourhamane Touré A., Tidjani A.D., Rajot J.L., Marticorena B., Bergametti G., Bouet C. *et al.* (2019) Dynamics of wind erosion and impact of vegetation cover and land use in the Sahel: a case study on sandy dunes in south-eastern Niger. *Catena*, **177**, 272–285.
- Ambouta J.M.K. & Dan Lamso N. (1996) *Rapport d'étude des sols des terroirs de Nazey et Togom (Ouallam)*. Faculté d'Agronomie, Université Abdou Moumouni de Niamey, Niamey, Niger, 30 pp.
- Arostegui J., Irabien M.J., Nieto F., Sangüesa J. & Zuluaga M.C. (2001) Microtextures and the origin of muscovite-kaolinite intergrowths in sandstones of the Utrillas Formation, Basque Cantabrian Basin, Spain. *Clays and Clay Minerals*, **49**, 529–539.
- Baosupee D., Massey A.J., Nazhad M. & Hubbe M.A. (2014) Heteroagglomeration as a mechanism of retaining CaCO₃ particles on the fibrils of cellulosic fines: A study by laser light diffraction and microscopy. *Colloids and Surfaces A: Physicochemical and Engineering Aspects*, **441**, 525–531.
- Barré P., Fernandez-Ugalde O., Virto I., Velde B. & Chenu C. (2014) Impact of phyllosilicate mineralogy on organic carbon stabilization in soils: incomplete knowledge and exciting prospects. *Geoderma*, **235–236**, 382–395.
- Bauluz B., Mayayo M.J., Yuste A. & González López J.M. (2008) Genesis of kaolinite from Albian sedimentary deposits of the Iberian Range (NE Spain): analysis by XRD, SEM and TEM. *Clay Minerals*, **43**, 459–475.
- Bauluz B., Yuste A., Mayayo M.J. & Canudo J.I. (2014) Early kaolinization of detrital Weald facies in the Galve Sub-basin (Central Iberian Chain, north-east Spain) and its relationship to palaeoclimate. *Cretaceous Research*, **50**, 214–227.
- Ben-Hur M. & Wakindiki I.I.C. (2004) Soil mineralogy and slope effects on infiltration, interrill erosion, and slope factor. *Water Resources Research*, **40**, W033031–W033038.
- Bergametti G., Marticorena B., Rajot J.L., Chatenet B., Féron A., Gaimoz C. *et al.* (2017) Dust uplift potential in the central Sahel: an analysis based on 10 years of meteorological measurements at high temporal resolution. *Journal of Geophysical Research: Atmospheres*, **122**, 12433–12448.
- Boski T., Pessoa J., Pedro P., Thorez J., Dias J.M. & Hall I. (1998) Factors governing abundance of hydrolyzable amino acids in the sediments from the N.W. European Continental Margin (47–50°N). *Progress in Oceanography*, **42**, 145–164.
- Boubacar M.M. (2016) *Caractérisation des stades de dégradation des écosystèmes de l'Ouest du Niger et proposition de techniques simples de restauration des stades dégradés*. Doctoral thesis. Université Abdou Moumouni de Niamey, Niger, 138 pp.
- Bui E.N. & Wilding L.P. (1988) Pedogenesis and mineralogy of a Halaquept in Niger (West Africa). *Geoderma*, **43**, 49–64.
- Chamley H. (1989) *Clay Sedimentology*. Springer Verlag, Berlin, Germany, 623 pp.
- Chorom M., Rengasamy P. & Murray R. (1994) Clay dispersion as influenced by pH and net particle charge of sodic soils. *Soil Research*, **32**, 1243.
- Cook H.E., Johnson P.D., Matti J.C. & Zemmels I. (1975) Methods of sample preparation and X-ray diffraction data analysis. Pp. 999–1007 in: *X-Ray Mineralogy Laboratory* (A.G. Kaneps, editor). Initial Reports of the DSDP. Printing Office, Washington, DC, USA.
- Coudé-Gaussen G. (1991) Les poussières sahariennes. Cycle sédimentaire et place dans les environnements et paléoenvironnements désertiques. John Libbey Eurotext, Paris. *Quaternary Research*, **39**, 485.
- Curtis C.D. (1990) Aspects of climatic influence on the clay mineralogy and geochemistry of soils, palaeosols and clastic sedimentary rocks. *Journal of the Geological Society*, **147**, 351–357.
- Daoudi L. (1996) *Contrôles diagénétique et paléogéographique des argiles des sédiments mésozoïques du Maroc; Comparaison avec les domaines atlantiques et téthysien*. Doctoral thesis. University of Marrakech, Marrakech, Morocco, 247 pp.
- Daoudi L., Ouajhain B., Rocha F., Rhouta B., Fagel N. & Chafiki D. (2010) Comparative influence of burial depth on the clay mineral assemblage of the Agadir-Essaouira basin (western High Atlas, Morocco). *Clay Minerals*, **45**, 453–467.
- Descroix L., Mahé G., Lebel T., Favreau G., Galle S., Gautier E. *et al.* (2009) Spatio-temporal variability of hydrological regimes around the boundaries between Sahelian and Sudanian areas of West Africa: a synthesis. *Journal of Hydrology*, **375**, 90–102.
- Dixon J.B. (1991) Roles of clays in soils. *Applied Clay Science*, **5**, 489–503.
- DMN (2015) *Annuaire statistiques, séries longues (1960–2015)*. Direction de la Météorologie Nationale, Niamey, Niger.
- Driessen P., Deckers J., Spaargaren O. & Nachtergaele F. (2001) *Lecture Notes on the Major Soils of the World*. World Soil Resources Reports, vol. 94. FAO, Rome, Italy, 334 pp.
- Duchaufour P. (1982) *Pedology: Pedogenesis and Classification*. Allen and Unwin, London, UK, 448 pp.
- Ducloux J., Guero Y. & Fallavier P. (1998) Clay particle differentiation in alluvial soils of southwestern Niger (West Africa). *Soil Science Society of America Journal*, **62**, 212–222.
- Ducloux J., Guero Y., Fallavier P. & Valet S. (1994) Mineralogy of salt efflorescences in paddy field soils of Kollo, southern Niger. *Geoderma*, **64**, 57–71.
- Ducloux, J., Guero, Y., Sardini, P. & Decarreau, A. (2002) Xerolysis: a hypothetical process of clay particles weathering under Sahelian climate. *Geoderma*, **105**, 93–110.
- Eberl D.D., Farmer V.C. & Barrer R.M. (1984) Clay mineral formation and transformation in rocks and soils. *Philosophical Transactions of the Royal Society of London. Series A, Mathematical and Physical Sciences*, **311**, 241–257.
- Elagib N.A., Zayed I.S. Al Saad S.A.G., Mahmood M.I., Basheer M. & Fink A.H. (2021) Debilitating floods in the Sahel are becoming frequent. *Journal of Hydrology*, **599**, 126362.
- Esquevin J. (1969) Influence de la composition chimique des illites sur leur cristallinité. *Bull. Cent. Rech. Pau-SNPA*, **3**, 147–153.
- Fagel N., Boski T., Likhoshway L. & Oberhaensli H. (2003) Late Quaternary clay mineral record in Central Lake Baikal (Academian Ridge, Siberia). *Palaeogeography, Palaeoclimatology, Palaeoecology*, **193**, 159–179.
- FAO (2014) *The State of Food Insecurity in the World 2014: Strengthening the Enabling Environment for Food Security and Nutrition*. Food and Agriculture Organization, Rome, Italy, 57 pp.
- Ferrell R.E., Aparicio P. & Forsman J. (2013) Interstratified clay minerals in the weathering environment. Pp. 115–139 in: *Interstratified Clay Minerals: Origin, Characterization and Geochemical Significance* (S. Fiore, J. Cuadros & F.J. Huertas, editors). AIPEA.

- Fofana B., Wopereis M.C.S., Bationo A., Breman H. & Mando A. (2008) Millet nutrient use efficiency as affected by natural soil fertility, mineral fertilizer use and rainfall in the West African Sahel. *Nutrient Cycling in Agroecosystems*, **81**, 25–36.
- Gavaud M. (1968) Les sols bien drainés sur matériaux sableux du Niger essai de systématique régionale. *ORSTOM*, **VI**, 278–307.
- Gavaud M., & Boulet R. (1967) *Carte pédologique de reconnaissance de la république du NIGER, échelle 1/500.000*. IGN.
- Gibbs R.J. (1977) Clay mineral segregation in the marine environment. *SEPM Journal of Sedimentary Research*, **47**, 237–243.
- Gourfi A., Daoudi L., Rhoujjati A., Benkaddour A. & Fagel N. (2020) Use of bathymetry and clay mineralogy of reservoir sediment to reconstruct the recent changes in sediment yields from a mountain catchment in the Western High Atlas region, Morocco. *Catena*, **191**, 104560.
- Guero Y. (1989) Les sols de la vallée du moyen Niger : organisation – tendance évolutive actuelle. *SOLSTROP*, **89**, 193–211.
- Guero Y. (2000) *Contribution à l'étude des mécanismes de dégradation physico-chimique des sols sous climat sahélien : exemples pris dans la vallée du Moyen Niger*. Thésis. Université Abdou Moumouni de Niamey, Niamey, Niger, 165 pp.
- Hartemink A.E. & Bockheim J.G. (2013) Soil genesis and classification. *Catena*, **104**, 251–256.
- Haynes R.J. & Naidu R. (1998) Influence of lime, fertilizer and manure applications on soil organic matter. *Nutrient Cycling in Agroecosystems*, **51**, 123–137.
- Heiri O., Lotter A.F. & Lemcke G. (2001) Loss on ignition as a method for estimating organic and carbonate content in sediments: reproducibility and comparability of results. *Journal of Paleolimnology*, **25**, 101–110.
- Herbillon A.J., Mestdagh M.M., Vielvoye L. & Derouane E.G. (1976) Iron in kaolinite with special reference to kaolinite from tropical soils. *Clay Minerals*, **11**, 201–220.
- Hulsemann J. (1966) An inventory of marine carbonate materials. *Journal of Sedimentary Petrology ASCE*, **36**, 622–625.
- Jaboyedoff M. (2001) Illite 'crystallinity' revisited. *Clays and Clay Minerals*, **49**, 156–167.
- Journet E., Balkanski Y. & Harrison S.P. (2014) A new data set of soil mineralogy for dust-cycle modeling. *Atmospheric Chemistry and Physics*, **14**, 3801–3816.
- Junge B. & Skowronek A. (2007) Genesis, properties, classification and assessment of soils in Central Benin, West Africa. *Geoderma*, **139**, 357–370.
- Kasanin-Grubin M. (2013) Clay mineralogy as a crucial factor in badland hill-slope processes. *Catena*, **106**, 54–67.
- Khormali F. & Abtahi A. (2003) Origin and distribution of clay minerals in calcareous arid and semi-arid soils of Fars Province, southern Iran. *Clay Minerals*, **38**, 511–527.
- Lang J., Kogbe C., Alidou S., Alzouma K.A., Bellion G., Dubois D. *et al.* (1990) The Continental Terminal in West Africa. *Journal of African Earth Sciences (and the Middle East)*, **10**, 79–99.
- Lebel T., Cappelaere B., Galle S., Hanan N., Kergoat L., Levis S. *et al.* (2009) AMMA-CATCH studies in the Sahelian region of West-Africa: an overview. *Journal of Hydrology*, **375**, 3–13.
- Liu Z., Colin C., Huang W., Le K.P., Tong S., Chen Z. & Trentesaux A. (2007) Climatic and tectonic controls on weathering in south China and Indochina Peninsula: clay mineralogical and geochemical investigations from the Pearl, Red, and Mekong drainage basins. *Geochemistry, Geophysics, Geosystems*, **8**, 5.
- Malam-Abdou M., Vandervaere J.-P., Bouzou-Moussa I., Descroix L., Mamadou I. & Faran-Maiga O. (2016) Genèse des écoulements sur deux petits bassins versants cristallins de l'Ouest du Niger: approche multi-échelles du fonctionnement hydrodynamique. *Géomorphologie: relief, processus, environnement*, **22**, 363–375.
- Malam Issa O., Valentim C., Rajot J.L., Cerdan O., Desprats J.-F. & Bouchet T. (2011) Runoff generation fostered by physical and biological crusts in semi-arid sandy soils. *Geoderma*, 167–168, 22–29.
- Mamadou I., Gautier E., Descroix L., Noma I., Bouzou Moussa I., Faran Maiga O. *et al.* (2015) Exorheism growth as an explanation of increasing flooding in the Sahel. *Catena*, **131**, 130–139.
- Mamoudou I. (2018) *Impact du climat et des activités anthropiques sur les écosystèmes dans le nord-ouest de la région de tillabéri au Niger*. Doctoral thesis. Université Abdou Moumouni de Niamey, Niamey, Niger, 133 pp.
- McFadden L.D., Wells S.G. & Dohrenwend J.C. (1986) Influences of quaternary climatic changes on processes of soil development on desert loess deposits of the Cima volcanic field, California. *Catena*, **13**, 361–389.
- McTainsh G. & Walker P. (1982) Nature and distribution of Harmattan dust. *Zeitschrift für Geomorphologie*, **26**, 417–435.
- Moberg J.P., Esu I.E. & Malgwi W.B. (1991) Characteristics and constituent composition of Harmattan dust falling in northern Nigeria. *Geoderma*, **48**, 73–81.
- Mohr E.C.J., Van Baren F.A. & van Schuylenborgh J. (1972) *Tropical Soils. A Comprehensive Study of Their Genesis*. Mouton, Den Haag, The Netherlands, 481 pp.
- Moore D. & Reynolds R.C. (1997) *X-Ray Diffraction and the Identification and Analysis of Clay Minerals*. Oxford University Press, New York, NY, USA 253 pp.
- Muhs D.R., Meco J., Budahn J.R., Skipp G.L., Simmons K.R., Baddock M.C. *et al.* (2021) Long-term African dust delivery to the eastern Atlantic Ocean from the Sahara and Sahel regions: evidence from Quaternary paleosols on the Canary Islands, Spain. *Quaternary Science Reviews*, **265**, 107024.
- Muller G. & Gatsner M. (1971) Chemical analysis. *Neues Jahrbuch für Mineralogie Monatshefte*, **10**, 466–469.
- Munroe J.S., Ryan P.C. & Proctor A. (2021) Pedogenic clay formation from allochthonous parent materials in a periglacial alpine critical zone. *Catena*, **203**, 105324.
- Negrão L.B.A. & da Costa M.L. (2021) Mineralogy and geochemistry of a bauxite-bearing lateritic profile supporting the identification of its parent rocks in the domain of the huge Carajás iron deposits, Brazil. *Journal of South American Earth Sciences*, **108**, 103164.
- Nguetnkam J.P., Kamga R., Villières F., Ekodeck G.E. & Yvon J. (2008) Altération différentielle du granite en zone tropicale. Exemple de deux séquences étudiées au Cameroun (Afrique centrale). *Comptes Rendus Geoscience*, **340**, 451–461.
- Noma Adamou S., Gourfi A., Abdourhamane Touré A. & Daoudi L. (2022) Érosion hydrique au sud-ouest du Niger: impacts des facteurs naturels et anthropiques sur les pertes en sols. *Géomorphologie: relief, processus, environnement*, **28**, 77–92.
- Obame R.M., Copard Y., Sebag D., Abdourhamane Touré A., Boussafir M., Bichet V. *et al.* (2014) Carbon sinks in small Sahelian lakes as an unexpected effect of land use changes since the 1960s (Saga Gorou and Dallol Bosso, SW Niger). *Catena*, **114**, 1–10.
- Omdi F.E., Daoudi L. & Fagel N. (2018) Origin and distribution of clay minerals of soils in semi-arid zones: example of Ksob watershed (Western High Atlas, Morocco). *Applied Clay Science*, **163**, 81–91.
- Panagos P., Borrelli P., Meusburger K., Yu B., Klik A., Lim K.J., Yang J.E. *et al.* (2017) Global rainfall erosivity assessment based on high-temporal resolution rainfall records. *Scientific Reports*, **7**, 4175.
- Paquet H. (1970) *Evolution géochimique des minéraux argileux dans les altérations et les sols des climats méditerranéens et tropicaux à saisons contrastées*. Mém. Serv. Carte géol. Als. Lorr., Strasbourg, France, 212 pp.
- Pédro G. (1984) Clay genesis in pedological conditions. Mineralogical, physico-chemical and hydric implication. Pp. 333–347 in: *Sciences Géologiques. Bulletin, tome 37, n°4, 1984. Minéraux argileux*. Persée, Lyon, France.
- Petschick R., Kuhn G. & Gingele F. (1996) Clay mineral distribution in surface sediments of the South Atlantic: sources, transport, and relation to oceanography. *Marine Geology*, **130**, 203–229.
- Pierre C., Bergametti G., Marticorena B., Abdourhamane Touré A., Rajot J.-L. & Kergoat L. (2014) Modeling wind erosion flux and its seasonality from a cultivated sahelian surface: a case study in Niger. *Catena*, **122**, 61–71.
- Pougnat R. & Greigert J. (1965) *Carte Géologique du Niger Occidental*. Échelle 1/2 000 000. Bureau de Recherches Géologiques et Minières, Orléans, France.
- Prospero J.M., Ginoux P., Torres O., Nicholson S.E. & Gill T.E. (2002) Environmental characterization of global sources of atmospheric soil dust identified with the Nimbus 7 total ozone mapping spectrometer (TOMS) absorbing aerosol product. *Reviews of Geophysics*, **40**, 2-1-2-31.
- Prospero J.M. & Nees R.T. (1986) Impact of the North African drought and El Niño on mineral dust in the Barbados trade winds. *Nature*, **320**, 735–738.
- Righi D. (1999) Pedogenic formation of kaolinite-smectite mixed layers in a soil toposequence developed from basaltic parent material in Sardinia (Italy). *Clays and Clay Minerals*, **47**, 505–514.

- Saffer D.M., Frye K.M., Marone C. & Mair K. (2001) Laboratory results indicating complex and potentially unstable frictional behavior of smectite clay. *Geophysical Research Letters*, **28**, 2297–2300.
- Shi X., Liu S., Fang X., Qiao S., Khokiattiwong S. & Kornkanitnan N. (2015) Distribution of clay minerals in surface sediments of the western Gulf of Thailand: sources and transport patterns. *Journal of Asian Earth Sciences*, **105**, 390–398.
- Singer A. (1980) The paleoclimatic interpretation of clay minerals in soils and weathering profiles. *Earth-Science Reviews*, **15**, 303–326.
- Singer A. (1984) The paleoclimatic interpretation of clay minerals in sediments – a review. *Earth-Science Reviews*, **21**, 251–293.
- Suzuki K., Matsunaga R., Hayashi K., Matsumoto N., Tabo R., Tobita S. & Okada K. (2014) Effects of traditional soil management practices on the nutrient status in Sahelian sandy soils of Niger, West Africa. *Geoderma*, **223–225**, 1–8.
- Suzuki K., Matsunaga R., Hayashi K., Matsumoto N., Tobita S., Bationo A. & Okada K. (2016) Long-term effects of fertilizer and organic matter application on millet in Niger. *Agronomy Journal*, **108**, 873–883.
- Traoré K., Blanchart P., Jernot J.-P. & Gomina M. (2007) Caractérisation physicochimique et mécanique de matériaux céramiques obtenus à partir d'une argile kaolinique du Burkina Faso. *Comptes Rendus Chimie*, **10**, 511–517.
- Velde B.B. & Meunier A. (2008) *The Origin of Clay Minerals in Soils and Weathered Rocks*. Springer, Berlin, Germany, 406 pp.
- Wakindiki I.I.C. & Ben-Hur M. (2002) Soil Mineralogy and texture effects on crust micromorphology, infiltration, and erosion. *Soil Science Society of America Journal*, **66**, 897–905.
- Wang C., Hong H., Li Z., Yin K., Xie J., Liang G. *et al.* (2013) The Eocene–Oligocene climate transition in the Tarim Basin, northwest China: evidence from clay mineralogy. *Applied Clay Science*, **74**, 10–19.
- Wang H., Liu Z.F., Sathiamurthy E., Colin C., Li J.R. & Zhao Y.L. (2011) Chemical weathering in Malay Peninsula and north Borneo: clay mineralogy and element geochemistry of river surface sediments. *Science China Earth Sciences*, **54**, 272–282.
- Zhang C. & Guo Z. (2014) Clay mineral changes across the Eocene–Oligocene transition in the sedimentary sequence at Xining occurred prior to global cooling. *Palaeogeography, Palaeoclimatology, Palaeoecology*, **411**, 18–29.